

Stress intensity factors for cracked plates under out-of-plane bending

M R Roy¹, J D G Sumpter¹, C M Timbrell² and M Wiehahn²

¹ QinetiQ, Rosyth Business Park, Dunfermline, KY11 2XR, UK

² Zentech Int. Ltd., 103 Mytchett Road, Camberley, Surrey, GU16 6ES, UK

Abstract: Stiffened plate structures such as ships and bridges often develop local stress concentrations which are a mixture of membrane tension and out of plane bending. Any cracks which initiate due to fatigue soon grow through the plating thickness. Modern steels are resistant to brittle fracture, but if cracks are left un-repaired, they may spread rapidly by fatigue. The rate of increase in fatigue crack length can be quantified using the elastic stress intensity factor, K .

Routines for the determination of K are available in ABAQUS, but they have limitations for performing extensive parametric studies on fatigue crack growth. Multiple fatigue crack tip positions must be analysed, requiring frequent re-meshing; and the crack direction and through thickness profile must be anticipated in advance. Zentech have developed the ABAQUS compatible software Zencrack specifically to deal with these problems.

This paper describes the problems of applying existing ABAQUS J integral methods to model cracks in structures under out-of-plane bending. Shell elements are shown to give path dependent and unreliable J values. Solid elements can be used, but the crack shape under fatigue cannot be easily predicted. Zencrack provides re-meshing techniques which allows the crack shape and speed of fatigue crack propagation to be efficiently predicted.

It is shown that Zencrack analysis overcomes ambiguities over how to take account of variations in K along the crack front in fatigue crack growth predictions. A set of results are presented which suggest that an out-of-plane bending stress is very much less detrimental for the fatigue life of a through thickness crack than a membrane stress of the same magnitude.

Keywords: finite element analysis, stress intensity factor, fatigue, ABAQUS, Zencrack.

1. Introduction

1.1 Basic fracture mechanics theory

Safety assessment of cracks requires a prediction of the future rate of fatigue crack growth. It is generally accepted that fatigue crack growth rate correlates with the severity of crack tip loading characterised by the elastic stress intensity factor, K . Handbook solutions (Murakami, 1986) for K are available for many standard configurations. However, finite element analysis has the advantage of providing case specific results which give a much closer simulation of structural loading and boundary conditions.

Once the stress intensity factor is known the fatigue crack growth rate can be predicted through the empirically derived relationship:

$$\frac{da}{dN} = C\Delta K^n \quad (1)$$

Where ΔK is the change in K during each fatigue cycle; da/dN is the increase in crack length per cycle; and C and n are experimentally derived constants. Since n is typically in the region of 3, an accurate determination of K is vital for reliable fatigue crack growth prediction.

Stress intensity solutions are normally expressed in non-dimensional form:

$$Y = \frac{K}{\sigma\sqrt{\pi a}} \quad (2)$$

Where σ and a are the characteristic stress and crack length respectively.

1.2 Application to ships

QinetiQ are working on a project (sponsored by the Sea Technology Group of the UK Ministry of Defence) dealing with the safety of cracks in ships. The aim is to provide ships' operators with guidance on the length of time for which a crack can be left without repair. This decision must balance the operational benefits of delaying a repair against the increased risk of failure. A crucial component in this decision is how quickly the crack extends with time at sea. As described above, this can be deduced from a knowledge of the stress intensity factor as a function of crack length.

Ships are large complex structures. It is impractical to inspect the structure in detail on a routine basis. Cracks are usually detected visually or by finding leakage. Most cracks appear in the main deck or in the side shell near the waterline. By the time they are detected they are typically right through the plate thickness and around 100 mm in length. Fortunately, peak stress levels in ships are such that critical crack sizes for failure are generally in the range of 500 mm and upwards (Kent, 2004). This calculation assumes the use of a reasonably tough steel, and may not hold for grade A steel at low temperature. Provided the assumption of good toughness can be justified, the issue of interest becomes the time taken for a fatigue crack to grow from 100 mm to 500 mm long. Typical plating thicknesses lie between 10 and 20 mm.

Factors such as welding distortion, lateral pressure, and intersection with bulkheads mean that a crack in a ship is likely to experience out-of plane bending as well as membrane tension. Figure 1 shows an idealization of the configuration of interest. The real structure will contain many further complexities involving out-of plane stiffening, but the geometry of Figure 1 in itself raises a number of difficulties which need to be addressed in a systematic manner before further complications can be introduced.

This paper discusses the following issues in relation to ABAQUS and the specialist fracture mechanics add-on package, Zencrack:

- use of shell elements to determine stress intensity factor;
- path dependence of J contour integral in shell elements;
- non-uniformity of stress intensity factors for 3D solid elements under out-of-plane bending;
- use of Zencrack to predict fatigue crack growth under combined tension and out-of-plane bending;
- influence of crack profile and degree of bending.

2. Characterizing cracks in shell elements

Efficient finite element analysis of large stiffened plate structures requires the use of shell elements. A typical mesh for a ship superstructure / deck intersection is shown in Figure 2. In principle it should be possible to determine K for this problem using the J contour integral calculation in ABAQUS. The J contour integral is linked to K through the relationship:

$$K = \sqrt{JE^*} \quad (3)$$

$$E^* = E \text{ for plane stress and } E^* = \frac{E}{1-\nu^2} \text{ for plane strain,} \quad (4)$$

where E is Young's modulus and ν is Poisson's ratio.

J is the elastic energy release rate expressed as a path independent line integral. The line integral approach is useful because J can be evaluated using stress, strain, and displacement parameters remote from the crack tip. This avoids the problem of trying to determine these values at the crack tip where they vary rapidly. The normal procedure is to take an average value of J from a number of contours and substitute into Equation 3 to determine K.

When this procedure was attempted for a crack at the deck to superstructure intersection in Figure 2, it was found to give a highly path dependent J with several negative values. The ABAQUS manual contains the warning that path dependence of J may occur with shell elements if there is

significant out-of-plane bending. It was surmised that this was the problem with the geometry of Figure 2.

It was decided to investigate stress intensity factor and fatigue crack growth under out-of-plane bending more systematically using the centre cracked plate geometry of Figure 1. The magnitude of the bending moment can be characterized in terms of the stress which it generates at each surface of the plate. The width of the plate is W ; its height H is three times its width; its thickness, t , is much less than W ($W/t > 50$); and it contains a central crack of length $2a$. The Young's modulus and Poisson's ratio were set at 207000 MPa and 0.3 respectively.

Figure 3 shows J/J_{average} plotted for the problem of Figure 1 analysed by thin shell elements (ABAQUS element S8R5). Figure 4 shows similar results for thick shell elements (ABAQUS element S8R). Both elements use a plane stress formulation. A uniform mesh of square elements having an in-plane dimension of $(2/3)t$ was used in the vicinity of the crack tip.

The J_{average} in Figures 3 and 4 is not an average of all 8 computed contours. Instead it is an average of the three consecutive contours which seem to give the most path independent J value and are hence judged most likely to give an accurate K . In principle, this shouldn't be a problem, since J should be path independent over all 8 contours. In practice, as shown in Figures 3 and 4, there is significant path dependence of J as soon as out-of-plane bending is introduced into the problem.

The advice in the ABAQUS manual is to discard only the contour nearest the crack tip when averaging J . This works well for the pure tension case, where it is only contour 1 which shows any significant deviation from J_{average} . However, for the pure bending case, it is not possible to identify any stable value of J (contours 3, 4, and 5 have been used to calculate J_{average}). The thick shell results (Figure 4) show similar behavior.

A major problem in interpreting results from the bending analysis is understanding how shell elements deal with the through thickness variation of stress intensity factor. Out-of-plane bending will produce tension on one surface of the plate and compression on the other. This should result in a stress intensity factor gradient through the thickness of the plate. In this circumstance it is not easy to understand the meaning of the single stress intensity factor generated by shell analysis.

3. Three dimensional analysis

Although it is impractical to carry out a global analysis of a whole ship using solid 3D elements, it is feasible to use such elements in a sub-model of the cracked region. It was decided to investigate the geometry of Figure 1 using C3D20R solid elements. One choice which then has to be made is how to treat the crack displacements on the compressive surface of the plate. If no boundary constraints are imposed, a negative stress intensity factor will be produced which is equal to the positive stress intensity factor on the tensile surface. Although mathematically correct, this is physically unrealistic, since the crack faces cannot in reality cross over each other. An alternative is to define frictionless contact between the two crack faces. This requires a model which represents both faces of the crack (if the faces are allowed to cross, a quarter plate model with symmetry at the crack plane can be used). A uniform mesh of elements with in-plane dimensions of $2/3t$ by $t/4$ through the thickness (four elements through the thickness) were used in the vicinity

of the crack tip. Stress intensity can be derived at each plane of nodes through the thickness, giving a gradation of K from the tensile to the compressive surface.

4. Stress intensity results

Tables 1 and 2 summarise the stress intensity results from the thin and thick shell analysis for a crack length of $2a = 100$ mm ($2a/W = 0.125$) in a centre cracked plate under a uniform tensile stress of 100 MPa. Results are also given for the same geometry subjected to an out-of-plane bending stress of 100 MPa, acting both alone, and in conjunction with the tensile stress.

Table 3 presents similar results for the solid 3D analysis.

Finally, Table 4 lists the non-dimensional stress intensity values for the different analyses for comparison with published analytical expressions (Murakami, 1986, Boduroglu, 1983). All the Y values in this table have been normalised by a stress of 100 MPa.

The following observations can be made:

- all of the element types give accurate Y values for pure tension. The solid element solution for pure tension is the average of K across the thickness, individual values being lowest at the surface and highest at the centre (Figure 5);
- under pure bending the shell element solution is much lower than that for the solid analysis. The latter corresponds with the analytical solution of (Boduroglu, 1983);
- two alternative solutions are given for the solid analysis. For the 'no contact' case, the crack faces cross, and negative K values occur on the compression side. This solution predicts higher values of K on the tension surface than the equivalent analysis with crack face contact (Table 3);
- the solid element solutions show correct superposition behavior (K values additive) for combined bending and tension (Table 3 and Figure 5). The shell element solutions do not (Table 1 and 2). There also seems to be an effect of the direction of bending in the shell analysis.

5. Analysis using Zencrack

The Zencrack software allows the direct simulation of fatigue crack growth. The crack is extended by an iterative process with a new mesh being generated automatically at each stage. The crack front is modelled by rings of elements with the innermost ring containing collapsed elements to represent the crack tip singularity.

When a crack has a stress intensity factor which varies from point to point along its surface it follows that the crack front will change its shape over the next growth increment. Ultimately, it might be expected that the crack will grow into an equilibrium, self-similar, profile; but this might not occur if it is growing into a changing stress field or approaching a free boundary.

The Zencrack approach was used to analyse the geometry of Figure 1 allowing the crack to grow through the plate by fatigue. The re-meshing of a fixed region to accommodate crack growth was discussed in (Cook, 1990). This technique uses a mapping technique to replace standard elements in an uncracked mesh with groups of brick elements, or a crack block, that contains a section of the crack front. Additional flexibility is added to this approach by allowing:

- shifting of the crack block boundaries;
- relaxation of surrounding elements;
- transfer of crack blocks from one location to another;
- use of large crack blocks to increase the volume in which crack growth may occur.

The above techniques are illustrated in Figure 5 of (Timbrell, 2004) as a side view of a 3D mesh. The analysis starts with a regular uncracked mesh. A crack block is inserted using the methodology of (Cook, 1990). The extent of crack growth that can be accommodated in this scheme will eventually be limited by element distortion. This can be overcome by adjusting the boundaries to produce well conditioned elements within a crack block region. There will then be some distortion outside of the crack block. This is resolved by an algorithm which allows the crack to grow in size by shifting the boundary and relaxing the surrounding region. Finally, the crack block is transferred to the next element. The combination of these techniques allows the crack front to travel through a mesh for most practical cases of interest.

6. Zencrack analysis of crack growth in a plate under bending

This section describes a Zencrack analysis of a centre cracked plate with $H/W = 1.5$ and an initially straight fronted crack of $2a/W = 0.23$ for four cases: pure tension (zero bending); 10% bending; 20% bending; and 40 % bending (i.e. membrane stress of 100 MPa plus an out-of-plane bending moment which gives a stress of ± 40 MPa).

Fatigue crack growth predictions are made using standard C and n constants for structural steel from (Yazdani, 1989):

$$C = 1.537 \times 10^{-9} \quad n = 3.344 \quad (5)$$

to give da/dN in mm/cycle for ΔK in $\text{MPa}\sqrt{\text{m}}$ in Equation 1.

As the crack extends in the Zencrack analysis it develops a curved profile. A typical finite element mesh developed by Zencrack to accommodate this curved profile is shown in Figure 6.

Figures 7 to 9 compare the Zencrack predicted development of crack front shape and corresponding distribution of Y at various $2a/W$ (measured on the compression face). Results are shown at three separate values of $2a/W$: 0.24, 0.5, and 0.75. Note that the crack takes a different number of cycles to reach a given $2a/W$ depending on the bending ratio. Results are shown at a corresponding $2a/W$ on the compression surface to allow the crack profiles to be compared. The crack extension axis is normalized by the surface crack extension under pure tension loading at

each $2a/W$. Figure 10 illustrates the development of the crack shape for each case; note that the crack has been allowed to grow to the edge of the plate, unlimited by fracture toughness.

The distribution of Y for a straight fronted crack (Figure 5) shows that, when bending is introduced, stress intensity is initially higher at the tensile surface and lower at the compressive surface compared to the pure membrane case. This causes the crack to grow faster at the tensile surface and initially more slowly at the compressive surface. This trend can be seen in Figure 7 where the crack in the 40% bending case extends faster at the more tensile surface. The shape of this profile alters the distribution of Y through the thickness, with an elevation of stress intensity factor at the re-entrant corner formed at the trailing edge at the compressive face. This compensates for the lower applied stress at that surface. The net effect is that the stress intensity becomes more uniform along the crack front.

Table 5 shows the relative life predictions for the four cases ("life" here is the number of cycles to reach $2a/W$ of 0.96 on the tension surface). The addition of 40% bending (100 MPa tension, ± 40 MPa bending) reduces the life by less than 10% compared to a pure tension stress of 100 MPa. This is much less than if the stress on the tensile surface had been used for the fatigue crack growth prediction. Assuming a pure tensile stress of 140 MPa would have reduced the predicted life by a factor of three compared to a tension stress of 100 MPa. This is not such an unlikely proposal, since prediction of fatigue crack initiation in codes such as BS7608:1993 is based on the surface stress including any local bending. Whilst this influences the propagation of a very small thumbnail crack, the Zencrack analysis shows that the rate of growth of the subsequent through thickness crack is largely dictated by the average membrane stress.

Attempts were made to run Zencrack for a greater degree of bending (50%). In this case the crack began to grow but the re-meshing routines were ultimately unable to cope with the crack shape which developed (Figure 11). This was due to the increasing acuteness of the crack front to the compression surface resulting in severe element distortion. Since hex elements are required at the crack front for J integral evaluation, it is difficult to see how a reasonable mesh could be developed to cope with extreme out-of-plane bending stress. Fortunately, most cracks in ships will experience less than 40% bending.

One curious issue which arises from a study of Figure 9 is that the stress intensity for 40% bending begins to adopt a progressively more non-uniform distribution across the thickness. The reasons for this are not yet understood as it was expected that the crack would try to grow into a shape which gave a uniform stress intensity. One reason could be that the crack is unable to reach a stable condition because of the effect of rapidly increasing Y at large $2a/W$.

7. Conclusions

Cracks in large stiffened structures such as ships are often subjected to out-of-plane bending loads. Efficient modelling of such structures requires the use of shell elements, which are not well suited to determine the stress intensity factors required for fatigue crack growth prediction.

It is noted in the ABAQUS manual that the J integral method for determination of stress intensity factor, K , is not suitable for use with shell elements. In theory, J should be path independent for all

contours not immediately adjacent to the crack tip. This was investigated using thick and thin shell elements. It was found that acceptably accurate values of K could be obtained in pure tension loading, but addition of out-of-plane bending caused significant path dependence of J , and uncertainty in the K value. It is concluded that cracks in structures where out-of-plane bending may occur can only be adequately modelled by using a 3D solid element sub-model.

An example calculation is presented for a centre cracked plate using C3D20R elements with four elements through the thickness. Assumptions on crack face interaction affect the resultant value of K , but the solutions appear to be well behaved with very little J path dependence. It is shown that, under bending, the stress intensity factor varies with position through the thickness. This implies that an initially straight crack front will not remain straight under fatigue growth (i.e. the crack will grow fastest where K is highest).

The ABAQUS add-on program Zencrack has been designed specifically to model this type of problem. Fatigue crack growth rate is calculated at each nodal point along the crack front and automatic re-meshing routines are used to move the crack forward to its new calculated position. Analysis of the centre cracked plate under bending problem with Zencrack shows that the crack grows into a curved profile leading on the tension surface. Combined tension and bending was modelled with a surface bending stress component of up to 40%. At 50% bending and beyond Zencrack was unable to successfully re-mesh the very acute corner at the trailing edge of the crack.

Although superimposed bending does reduce the fatigue life, the effect is much less dramatic than if the same stress increase had been applied as membrane tension. For instance, increasing the membrane stress by 40% would reduce the fatigue life to only one third of its previous value. In contrast, adding the 40% enhancement as a bending stress is predicted to reduce the fatigue life by less than 10%.

8. References

1. Boduroglu, H. and Erdogan, F., "Internal and Edge Cracks in a Plate of Finite Width Under Bending," *Journal of Applied Mechanics*, Vol 50, 621-629, 1983.
2. BS7608:1993 "Fatigue Design and Assessment of Steel Structures."
3. Cook, G., Timbrell, C., Claydon, P. W., "Automatic and Adaptive Finite Element Mesh Generation for Full 3D Fatigue Crack Growth," *Struceng and Femcad conference*, Grenoble, France, 1990. Available at http://www.zentech.co.uk/zencrack_papers.htm.
4. Kent, J. S. and Sumpter, J. D. G., "Probability of Brittle Fracture for a Cracked Ship," presented at ASRANET symposium, Barcelona, July 2004.
5. Murakami, Y., "Stress Intensity Factors Handbook," Pergamon Press, 1987.
6. Timbrell, C., Chandwani, R., Cook, G., "State of the Art in Crack Propagation," *Journee scientifique, Les methodes de dimensionnement en fatigue*, Available at http://www.zentech.co.uk/zencrack_papers.htm.
7. Yazdani, N., and Albrecht, P., "Crack Growth Rates of Steel in Air and Aqueous Environments," *Engineering Fracture Mechanics*, Vol 32, No 6, pp 997-1007, 1989.

9. Tables

Table 1. Stress intensity factors for thin shell analysis.


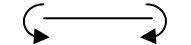
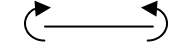
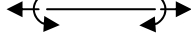
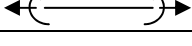
Configuration	K combined (MPa \sqrt{m})	K tensile (MPa \sqrt{m})	K bending (MPa \sqrt{m})
	-	40.0	-
	-	-	12.3
	-	-	12.3
	32.2	As above	-7.81
	50.2	As above	10.2

Table 2. Stress intensity factors for thick shell analysis.

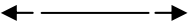
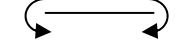
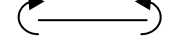

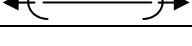
Configuration	K combined (MPa \sqrt{m})	K tensile (MPa \sqrt{m})	K bending (MPa \sqrt{m})
	-	39.1	-
	-	-	13.2
	-	-	13.2
	32.1	As above	-7.0 (inferred)
	49.1	As above	10.0 (inferred)

Table 3. Stress intensity factors for 3D solid analysis.

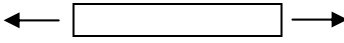


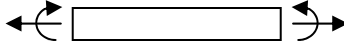
Configuration	K combined (MPa \sqrt{m})	K tensile (MPa \sqrt{m})	K bending (MPa \sqrt{m})
	-	36.4 (surface) 40.1 (average)	-
 NO CONTACT	-	-	27.4 (surface)
 CONTACT	-	-	22.3 (surface)
	64.0 (surface)	36.4	27.6 (inferred at surface)

Table 4. Non-dimensional stress intensity geometry factors compared to analytical solutions.

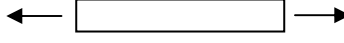


Configuration	Y Shell	Y 3D solid	Y Analytical
	1.01	1.01 (average)	1.01
 NO CONTACT	0.31	0.66	0.65
 CONTACT	-	0.54	-

Table 5. Effect of bending stress on fatigue life.

Case	Fatigue life - % pure tension
10% bending	99.4%
20% bending	96.9%
40% bending	91.3%

10. Figures

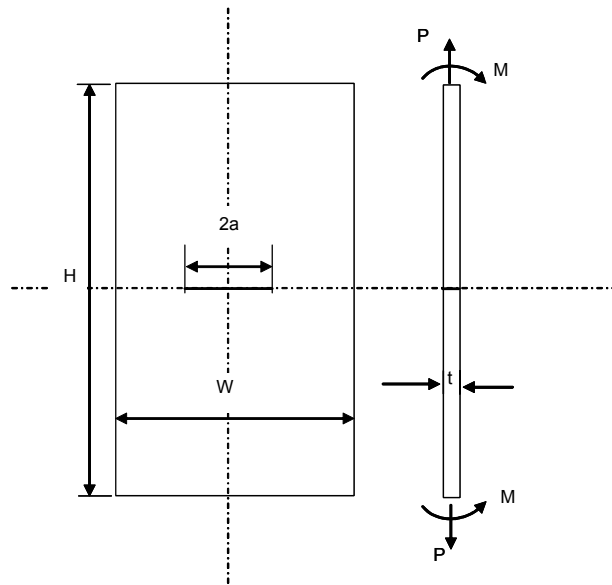


Figure 1. Centre cracked plate under combined tension and out-of-plane bending.

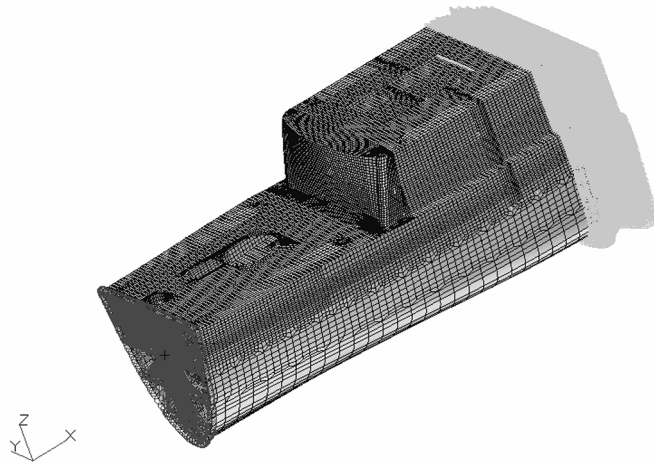


Figure 2. Section of ship and superstructure modelled with shell elements.

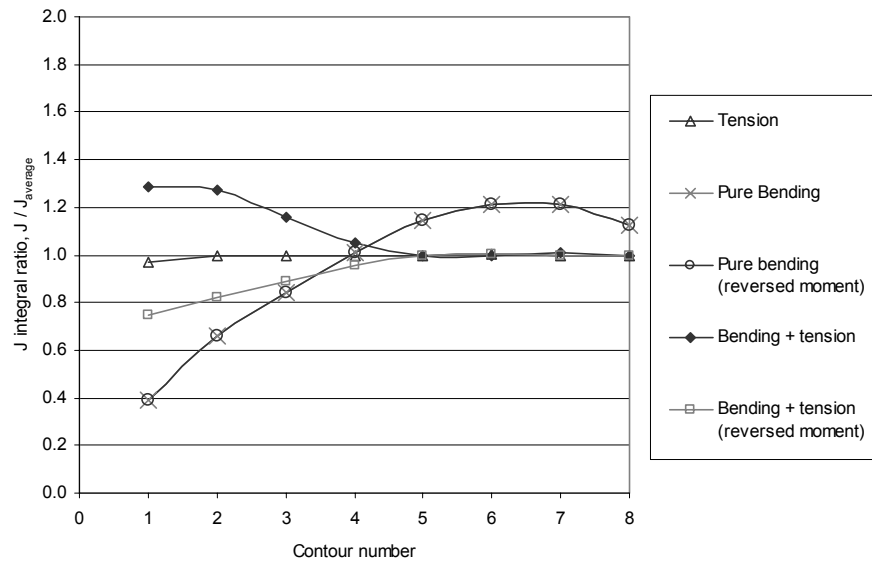


Figure 3. Path dependence of J integral for ABAQUS thin shell analysis.

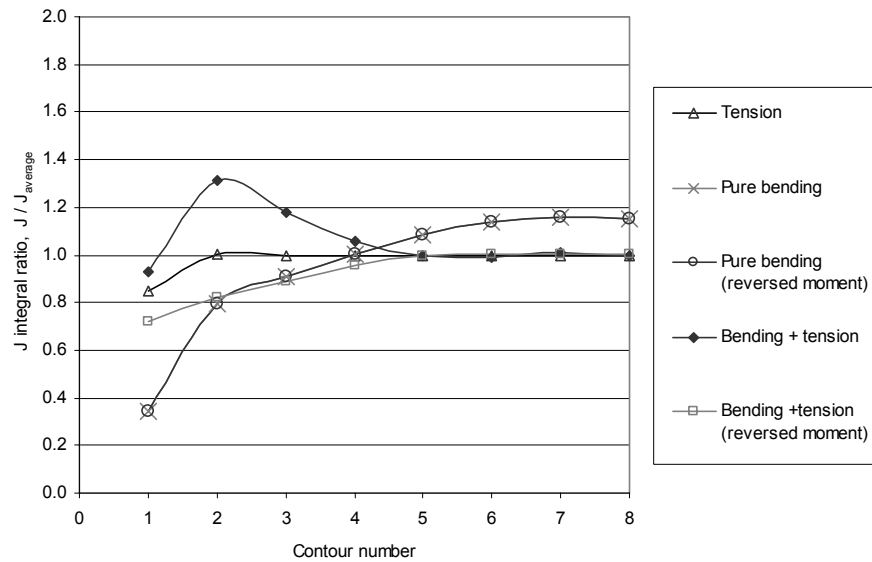


Figure 4. Path dependence of J integral for ABAQUS thick shell analysis.

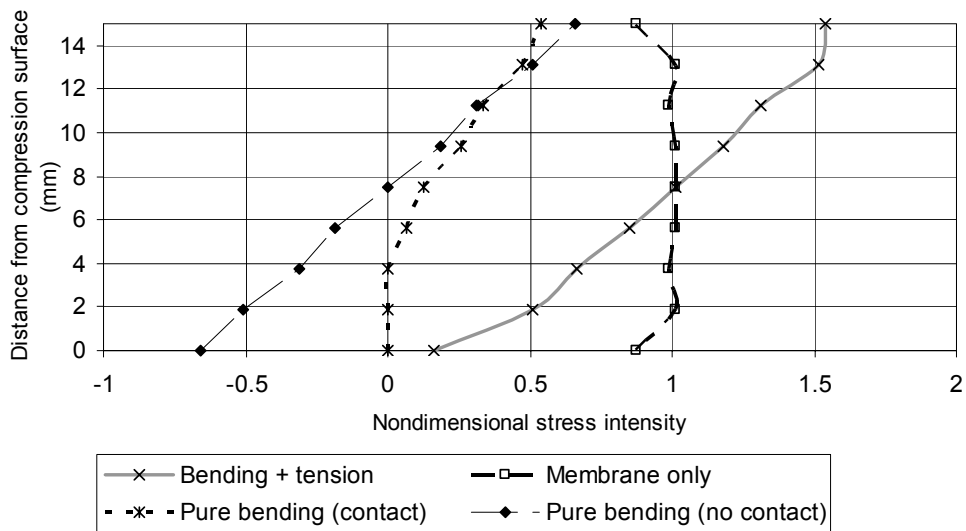


Figure 5. Distribution of Y through thickness for ABAQUS 3D solid analysis. Straight crack front.

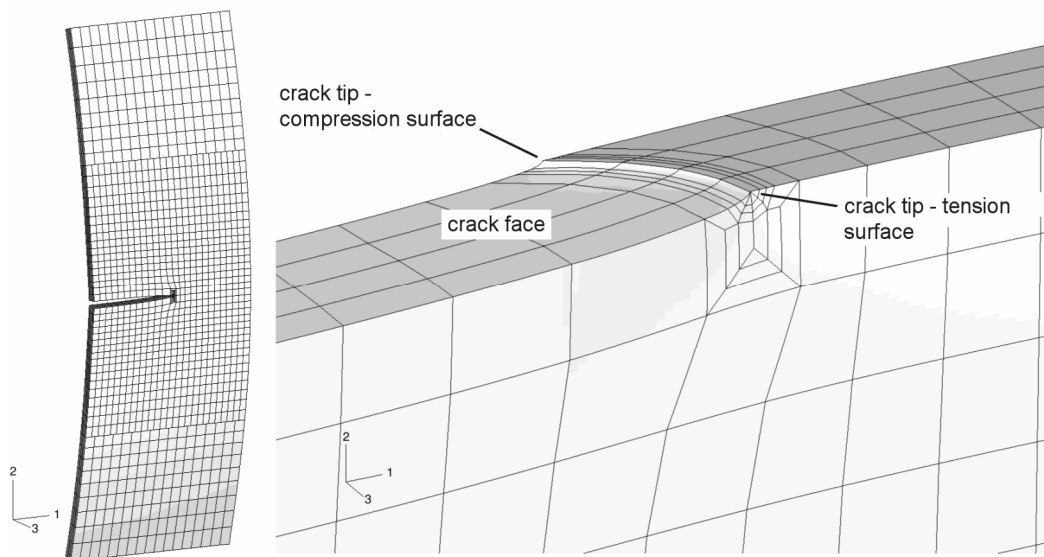


Figure 6. Displaced shape of 40% bending case, after 24 Zencrack analysis increments, showing detailed mesh developed at crack tip

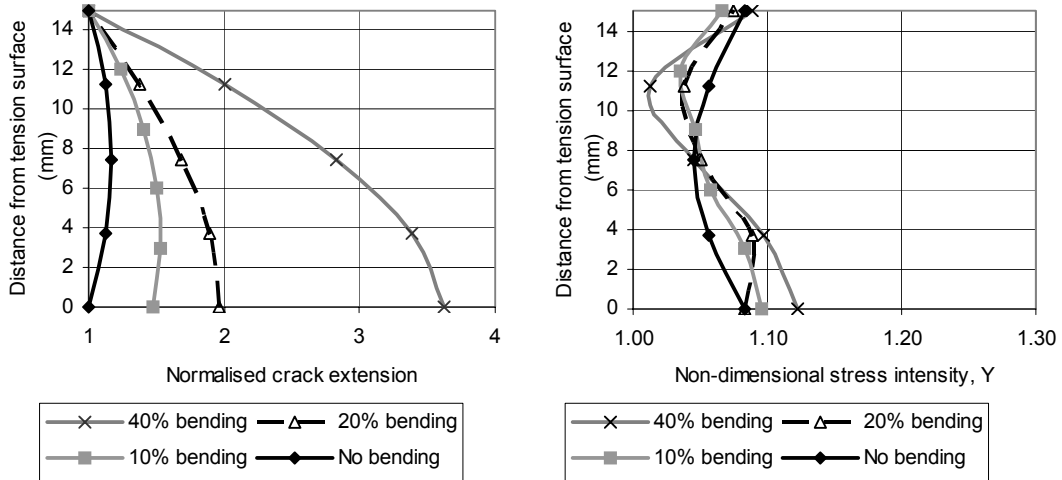


Figure 7. Crack profile and distribution of Y from Zencrack analysis at $2a/W = 0.24$.

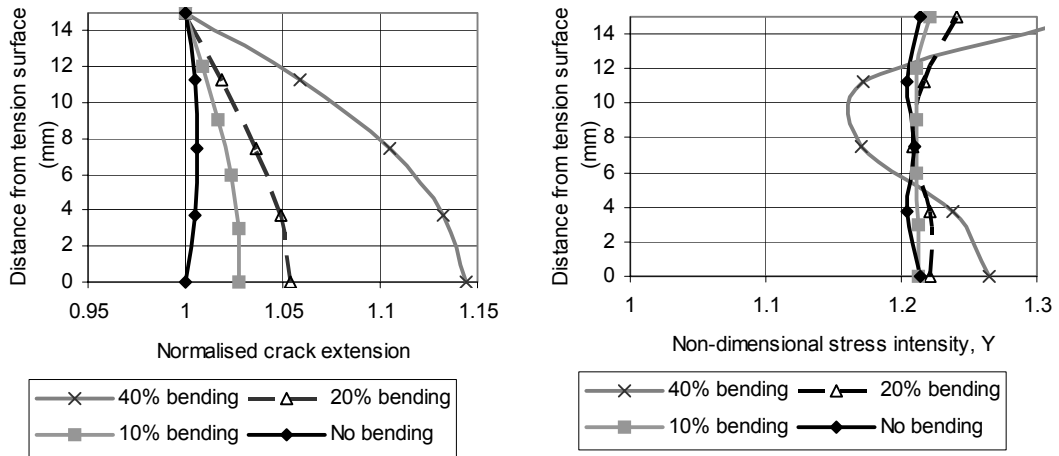


Figure 8. Crack profile and distribution of Y from Zencrack analysis at $2a/W = 0.5$.

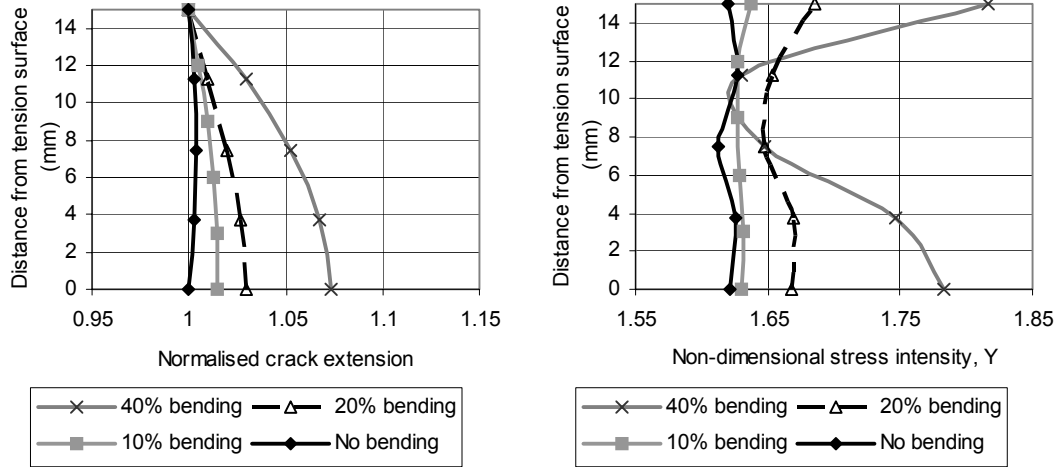


Figure 9. Crack profile and distribution of Y from Zencrack analysis at $2a/W = 0.75$.

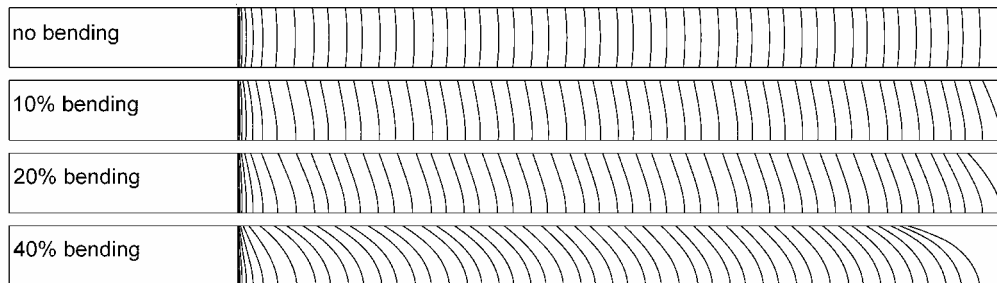


Figure 10. Successive crack front profiles for different degrees of bending



Figure 11. Successive crack front profiles for 50% bending case